Traces of impact in crystalline rock

A summary of processes and products of shock metamorphism in crystalline rock with focus on planar deformation features in feldspars

Fredrika Svahn

Dissertations in Geology at Lund University,
Bachelor's thesis, no 391
(15 hp/ECTS credits)

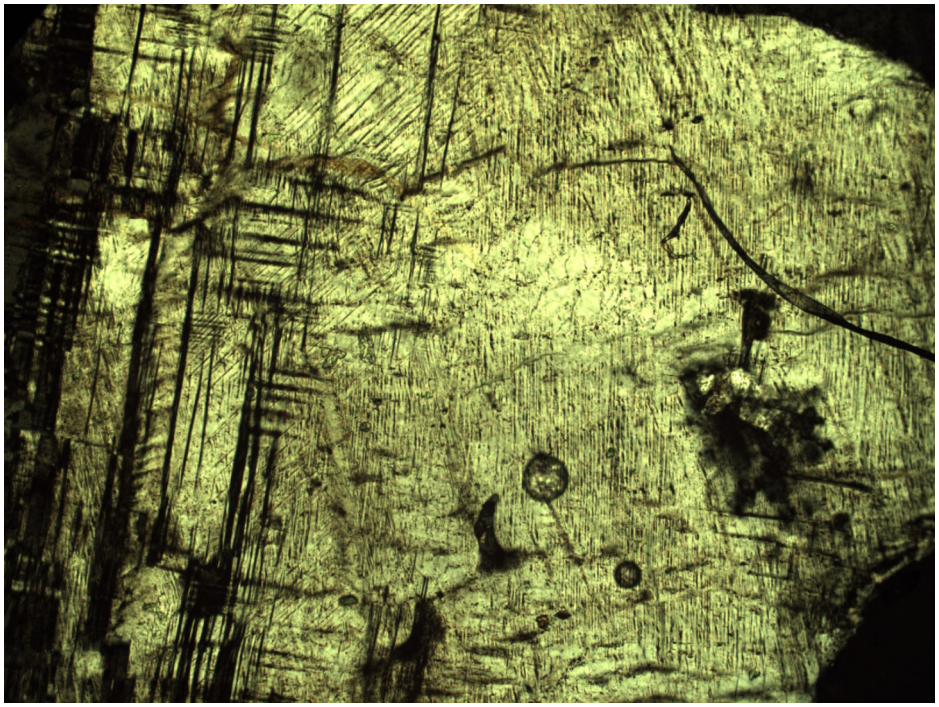

Department of Geology
Lund University
2014

Traces of impact in crystalline rock

A summary of processes and products of shock metamorphism in crystalline rock with focus on planar deformation features in feldspars

Bachelor's thesis

Fredrika Svahn

Department of Geology
Lund University
2014

Contents

Cover Picture: Microscopic deformation features in k-feldspar grain. Photomicrograph (crossed polars). Photo: Fredrika Svahn

Traces of impact in crystalline rock- A summary of processes and products of shock metamorphism in crystalline rock with focus on planar deformation features in feldspars

FREDRIKA SVAHN

Svahn, F., 2014: Traces of impact in crystalline rock- A summary of processes and products of shock metamorphism in crystalline rock with focus on planar deformation features in feldspars. *Dissertations in Geology at Lund University*, No. 391, 22 pp. 15 hp (15 ECTS credits).

Abstract: Shock metamorphic features have been identified in alkali feldspars within granitic rock samples from the Siljan impact structure in Sweden. Observed features include deformation bands, ladder textures, "V-textures" planar fractures, "long deformation features", and true planar deformation features (PDFs). The studied samples are of the same lithology but come from different shock pressure intervals and the results vary for samples within different pressure intervals. The majority of the deformation features have been observed in the sample from the highest shock pressure interval; 15-20 GPa. Long deformation features and planar deformation features are the only two deformation features observed in samples from the lower shock pressure interval 10-15 GPa. A much higher frequency of deformation structures have also been observed in the sample derived from the highest pressure interval.

Keywords: impacts, shock metamorphism, crater formation, shock metamorphic features, planar deformation features, alkali-feldspars, Siljan impact structure.

Supervisor: Sanna Alwmark

Subject: Bedrock Geology

Fredrika Svahn, Department of Geology, Lund University, Sölvegatan 12, SE-223 62 Lund, Sweden. E-mail: geo10fsv@student.lu.se

Spår av impakt i kristallin berggrund - En sammanfattning av processer och produkter relaterade till chockmetamorfos med särskild fokus på deformationsstrukturer i fältspater

FREDRIKA SVAHN

Svahn, F., 2014: Spår av impakt i kristallinberggrund– En sammanfattning av processer och produkter relaterade till chockmetamorfos med särskild fokus på deformationsstrukturer i fältspater. *Examensarbeten i geologi vid Lunds universitet*, Nr. 391, 22 sid. 15 hp.

Sammanfattning: Chockmetamorfa strukturer i alkalifältspater har genom studier i polarisationsmikroskop identifierats i graniter från Siljan- nedslagskrater. De mikroskopiska strukturer som observerats omfattas av; deformation bands, ladder textures, planar fractures, ”long deformation features", samt planar deformation features (PDFs). Stufferna härstammar från samma bergart, Järna graniten, från olika tryckintervaller inom siljankratern. Studiens resultat varierar för prover från olika tryckintervall, en avsevärd större mäng deformations strukturer återfanns i provet som beräknas tillhöra det högsta tryckintervallet 15-20 GPa. Long deformation features och Planar deformation features är de enda deformations strukturer som observerats i prover från det lägre tryckintervallet 10-15 Gpa. Provet från det högsta tryckintervallet visade sig även innehålla en mycket större diversitet av deformationsstrukturer.

Nyckelord: impakt, chockmetamorfos, kraterformation, chockmetamorfa strukturer, plana deformations strukturer, alkalifältspater, Siljan nedslagskrater.

Handledare: Sanna Alwmark

Ämnesinriktning: Berggrundsgeologi

Fredrika Svahn, Geologiska institutionen, Lunds universitet, Sölvegatan 12, 223 62 Lund, Sverige. E-post: geo10fsv@student.lu.se

1 Introduction

When a celestial body collides with Earth's surface, the kinetic energy will be instantly transferred to the target rock through so-called shockwaves. These shock waves exert extremely high pressures to the surrounding material. Maximum shock pressures can reach up to over 100 GPa at the point of impact (Stöffler 1971). Depending on the level of pressure the shock waves exerts on the target material, different levels of deformation will be recorded in the target material. The level of deformation can range from complete melting and evaporation closest to the point of impact, to microscopic alterations in the crystal structure of individual mineral grains.

This paper focuses specifically on microscopic features formed upon impact. They are especially interesting since several of these shock metamorphic deformation features can only be found in rocks that have been exposed to high-energy shock waves, which are only produced naturally by impact events. Therefore some of these features have been excessively studied (Stöffler & Langenhorst 1993; Grieve et al. 1995), originally because they could be used as proof of an actual impact event (Stöffler 1971). Some features have later proven to be useful when determining the level of shock pressure exerted at different areas within an impact crater. The aim of this study is to investigate the occurrence of shock metamorphic features in K-feldspars from the Siljan impact structure, Sweden.

Microscopic deformation features created by shock metamorphism in feldspars have not been as closely studied as those found in quartz. One reason for this is that feldspars are more prone to weathering and secondary alteration, which make them less durable than quartz. Another reason is that quartz is uniaxial whilst feldspars are biaxial, which in a purely optical way, makes quartz easier to study. Further, quartz and feldspars are usually found together in the target rock of most studied impact craters, which is yet another reason to why feldspars have been largely overlooked when it comes to detailed studies of shock metamorphic features. A majority of the studies of shock features in feldspars has been carried out as laboratory experiments (Stöffler 1974; Robertson 1975; Ostertag 1983 etc.). Gaining better knowledge of the way feldspars respond to different shock pressures will be useful when studying rocks with a low quartz concentration and especially when focusing on extraterrestrial material since they are essentially devoid of quartz. Further studies will ultimately be a valuable addition to the already well-known spectra of shock deformation features in quartz.

2 Crater formation

When a large body strikes Earth, the high energy collision will affect a large volume of rock in the impact area. The surface material near the point of impact will be highly deformed and dislocated by the immense forces released upon impact. The collision between a large body and an even larger target results in the formation of an impact crater. Impact crater formation is a fast and continuous process. The process begins at the moment the projectile reaches the target surface and ends, according to Melosh (1989), "when things stop falling". The tremendous amounts of energy released when a large body collides with an even larger target generate a complex assemblage of intermingling forces resulting in extensive physical alterations of the target and often complete destruction of the projectile.

2.1 Crater forming processes

The types of impact craters that will be discussed in this chapter are those formed during collision with a high-velocity projectile. These impact craters are called hypervelocity impact craters, and should not be confused with structures formed by smaller projectiles. The behaviour of bodies travelling through the Earth's atmosphere varies depending essentially on the size and constitution of the body (French 1998). A body of a few meters or smaller, will not survive the forces exerted by the atmosphere and will subsequently break up and lose most of its original velocity. Upon impact a smaller projectile will rarely travel faster than a few meters per second (French 1998). These kinds of impacts normally form relatively shallow depressions with a diameter rarely exceeding the width of the original impactor, which can often be found intact at the bottom of the cavity (French 1998). On the contrary, a more massive body, normally larger than 20m can, if sufficiently coherent, survive the traverse through the atmosphere without loosing much of its original speed. Consequently, a large solid body will strike the target surface with velocities exceeding 11km/s, resulting in the formation of a hyper-velocity impact crater (French 1998).

The formation of a crater begins almost instantaneously at the moment of collision (French & Koeberl 2010). The kinetic energy of the striking projectile is transferred into the target rock whereupon transient high-energy shockwaves are generated (French & Koeberl 2010). These shockwaves will radiate in an elliptical path from the point of impact through the target rock with extremely high velocities, some times up to 10km/s (French 1989). The wave's amplitude will decrease as it reaches further away from the point of impact, degrading into a stress wave, (Fig. 1; Melosh 1989) and finally transforming into a seismic wave (French & Koeberl 2010). When the shockwaves extend to the surface of the target rock, large amounts of material will be launched from its original position (French 1998), and is later deposited either back into the crater as crater-fill breccias or as ejecta-debris at various distances from the crater (French & Koeberl 2010). Although the immediate formation of hypervelocity impact craters is a continuous and extremely

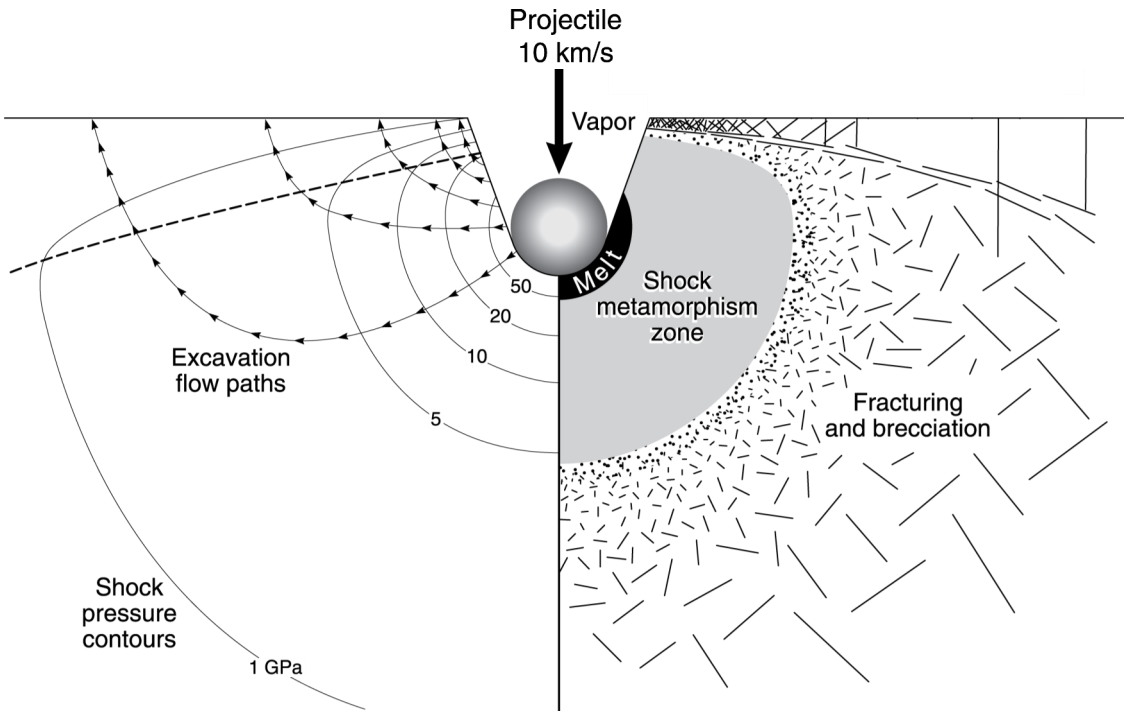

Fig. 1. Peak pressure- and deformation zones in target rock. Figure illustrating processes active during contact/compression stage. Peak shock pressures are indicated by pressure isobars in the left-hand side of the figure. The right-hand side shows deformation zones within the target rock. The area closest to the point of impact consists of melted and vaporized material. Further out at shock pressures <50 GPa the shock metamorphism zone is found. Within this zone most shock-features are created. Further out from the point of impact fractures and brecciated rocks are created. It is important to note that this is not the final stage of the cratering process and the distribution of shock metamorphosed material will not remain in their original positions at the end of the excavation stage. The dashed arrows indicate general paths for material movement during excavation where a large part of the shocked target rock will be mixed and displaced. Figure modified from French 1998.

rapid process, the formation process is often split into three stages (French 1998).

These stages called; **Contact/compression, excavation** and **modification,** separate the different physical processes involved in the cratering process (Gault et al.1968).

Below follows a short description the three stages of crater formation. For an illustrated summary of the crater formation process, see Fig. 2.

2.1.1 Contact/compression stage:

The contact/compression stage only lasts for a very brief period, just a little more than a second for the largest impacts (Melosh 1989). This primary stage is initiated at the moment the striking body comes in contact with the target surface and ends at the moment the projectile is completely unloaded.

The dominating processes involved in this stage are; the expansion of shockwaves, followed by the release- or rarefaction waves.

As the incoming projectile reach the target surface, the target material will be accelerated while the striking body will be decelerated (Melosh 1989). Given the target is composed of solid rock, the striking body will only penetrate about 1-2 times its own diameter into the target (French 1998).

The great difference in velocity between the two bodies will give rise to a system of shock waves. These shock waves form at the boundary between compressed and uncompressed material (Melosh 1989), and work to transfer the kinetic energy of the projectile into the target rock (Gault et al. 1968).

Two separate shock wave fronts, generated at the point of impact, will be travelling in nearly opposite directions (Melosh 1989). Firstly one front will propagate into the target rock in a crescent shaped path (Fig.1,2), secondly another wave front will travel up the projectile itself (Gault et al. 1968). The shockwaves that were directed down into the ground will compress the material at extremely high pressure in the area closest to the contact point, normally leading to melting and/or vaporization of the target material (French 1998). The properties and nature of the compressive shock wave are originally relatively simple. However while advancing through a heterogeneous target rock, the shock wave will be extensively altered, becoming increasingly more complex and distorted (Rinehart 1968).

As it radiates through target material the speed and energy of the shock wave will be drastically reduced.

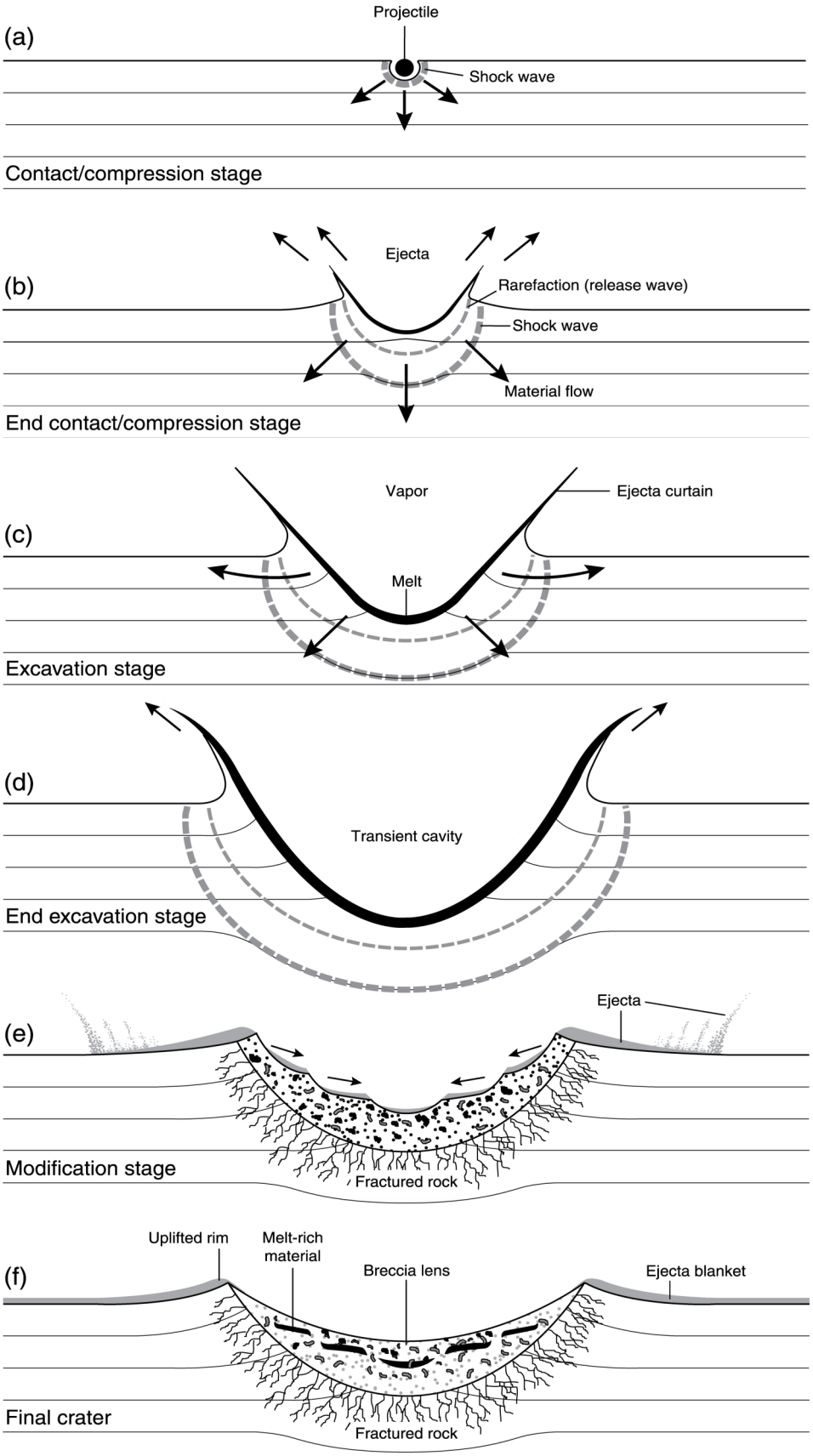

Fig. 2. Formation of a simple impact structure. The illustration summarizes the three stages of the crater forming process. From French 1998.

The energy loss is partly due to the dilution of the energy density when the wave spreads out over an increasingly larger volume (Gault et al.1968). Energy is also transferred to the target rock through acceleration, heating and deformation (French 1998).

Since the pressure exerted on the target rock is decreased with increasing distance from the impact point, the area surrounding the point of impact will consist of elliptical zones with varying peak pressure levels, ranging from >100 GPa near the initial point of impact to ≤2 GPa at the crater rim area (Fig. 1; French 1998)

The compressive wave front that moved up the length of the projectile, subjecting the projectile material to extremely high pressure (Melosh 1989), will eventually reach the back end of the projectile. Upon reaching the free surface at the very back of the body the compression front will be replaced by a release- or rarefaction wave. This rarefaction wave moves in the opposite direction of the initial shock wave front (Gault et al. 1968). Passing through the recently compressed material of the projectile the rarefaction wave will decompress the highly shocked material, which will ultimately lead to the complete melting and/or vaporization of the entire projectile (Melosh 1989; French 1998).

When reaching the surface of the target rock, the release wave continues in the path of the original downwards-moving shock front, continuing to release the target rock. The contact/compression stage is considered to end at the moment the release wave reaches the surface of the target rock and the projectile is completely unloaded (Melosh 1989).

2.1.2 Excavation stage

During the excavation stage the target material within the affected area is ejected from the crater due to the combined forces of shock- and release waves (Gault et al.1968). The transportation of material from the crater area is the process responsible of forming the characteristic depression connected to impact structures.

The excavation stage is initialized upon the arrival of the rarefaction wave from the projectile to the original contact point. At this time the projectile is completely unloaded, and does no longer play any part in the crater forming process (French 1998).

Upon entering the target rock, the rarefaction wave will continue to release the compressed material as it enters the target rock, leading to melting and vaporization of the areas exposed to the highest amount of pressure (French & Koeberl 2010).

Additional release waves will be generated as upwards-directed shock waves encounter the ground surface of the target rock (Melosh 1989). These rarefaction waves have a downward direction and will vaporize, melt, break or distort the target rock as they pass (Melosh 1989). The level of deformation the target rock will experience depends on what degree of shock compression the material was initially exposed to (Fig. 3; French 1998).

The excavation stage is mainly driven by two dominating processes; the expansion of shock waves and the excavation flow (Melosh 1989). Excavation flow refers to the transport of material that is initiated during this stage. The movement is driven by kinetic energy that is released when the rarefaction waves unload the target material. The kinetic energy drives large amounts of target rock outwards and upwards from the impact zone. Ultimately, the excavation flow is the mechanism that physically digs out the crater (Melosh 1989).

2.1.3 Modification stage

This final phase of the crater formation begins as the excavation flow ceases and the newly formed crater has reached its maximum diameter (Melosh 1989). In crater modeling there is a supposed stage of balance at the moment when the shock- and release waves no longer affect the crater area, right before the modification stage begins (French 1998).

The modification stage of the crater formation process is driven by natural geological mechanisms like gravity and rock mechanisms (French 1989). The modification stage is most prominent during the moments closely following the end of the previous excavation stage (Melosh 1989).

The gravitational forces and rock mechanics cause collapsing of crater walls and material flow down the sides of the crater (Melosh 1989).
There is no definite way to determine when the modification stage ends and normal geological processes begins (French 1989).

The morphology of the final impact crater depends largely on the constitution and composition of the target rock as well as the size, velocity and composition of the impactor. Angle of impact and gravitational circumstances also play a role in shaping the impact crater. There are several different variations of impact structures, such as; simple-, complex and multi-ring-craters.

3 Shock metamorphism of rocks and minerals

In the early 1960's an earlier unknown form of rock deformation, connected exclusively to impact sites, was discovered. This type of deformation was found to be generated by the high-pressure shock waves connected to impact events and came to be called shock- or impact metamorphism (Stöffler 1971).

Shock metamorphic features are the result of the fact that the physical properties of rock material that is introduced to shockwaves with amplitudes exceeding the target rock's dynamic elastic limit, Hugoniot elastic limit. The elastic limit will change upon release from the highly elevated pressure- and temperature levels (Stöffler 1971).

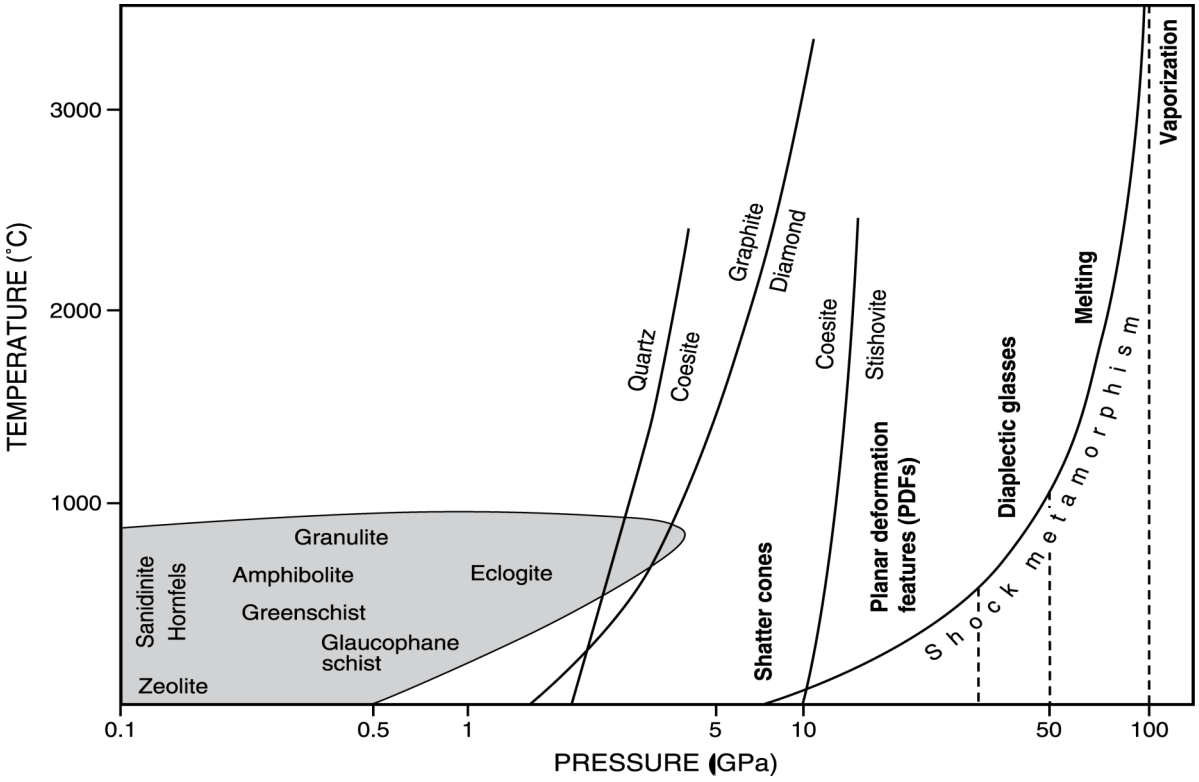

Fig. 3. Conditions of shock–metamorphism. P–T plot illustrating pressure and temperature required for development of various shock-metamorphic deformation features. X-axis showing pressure in gigapascal (logarithmic scale) and y-axis showing temperature in degrees Celsius. For comparison, a plot of metamorphic facies connected to conventional endogenic deformation (grey zone to the left in the diagram, pressures below 0.5 GPa). The zone where permanent shock metamorphic features develop, can be seen to the right, approximately <7 to 100 Gpa.
The line "Shock metamorphism" indicates the post shock temperatures produced by varying levels of shock pressure in crystalline rock. Figure modified from French 1998

The total range of shock pressure wherein permanent shock effects can be induced in a mineral is determined by the mineral's individual elastic limit and its specific melting point. For quartz the pressure range is between 5 GPa to >50 GPa (Stöffler & Langenhorst 1993).
The highly rapid passage of the shock- and release wave, generate extremely high strain rates, transient stress conditions and temperatures that cannot be produced during normal geological processes. (French 1998).

As a shock wave spreads through the target rock it loses energy. The peak pressure levels exerted on the rock material will therefore lessen further from the point of impact. For this reason the target rock within an impact crater will experience different energy levels and subsequently, different levels of deformation. The area around the point of impact can be divided into zones of different peak shock pressures, (Fig. 1).

Through field studies and laboratory experiments, variations within some deformation features have been connected to different levels of peak pressure (Fig. 3). for a plot of common shock deformation features connected to different levels of peak pressure.

3.1 Impactites

The term impactite will in this paper will be used the same way as in French 1998. Impactite refers to "all rocks affected- or produced by, the shock waves and other processes generated by hypervelocity meteorite impact events" (French 1998).
Because of the many different forces and mechanisms acting, to different extent, on a large volume of homogenous material, the final products of an impact will be highly variable. The physical characteristics of an impactite will differ depending on several variables such as original lithology of the target rock, and amount of pressure and temperature exerted on the rock material. The different types of impactites will form at varying locations and during different stages throughout the crater formation process. The final distribution of various impactites is determines by the mechanisms of the excavation flow and subsequent modification (French 1998).

Impactites can be found inside (allogenic), around (ejecta) or under (parautochthonous), an impact crater. The allogenic rocks that can be found inside the crater, and as ejecta outside the crater rim, are usually composed of breccias and melts. Breccias found inside the crater are usually complex collections of rock fragments from various locations, with a largely varying

shock pressure history. The parautochthonous rocks found underneath the crater floor are usually more or less intact. Shatter cones and other shock metamorphic features are typical features of these rocks (French 1998).

3.2 Shock metamorphic features

Traces of an impact can be found as a collection of shock metamorphic features. The characteristics of these features are determined by pressure level and post shock temperature exerted on the specific mineral in which the features were produced (French 1998). Many of these deformation features, although formed under extreme conditions are very similar to structures formed during 'normal' geological processes and can therefore not be used as proof of an impact event (French & Koeberl 2010). However there are features that have been found to form exclusively in connection to high-pressure shock waves, making them unequivocal proof of impact (Stöffler 1971).

Shock metamorphic features vary in form and size, and can be found on both microscopic- as well as megascopic scales (French 1998).

3.3 Megascopic features

Megascopic features are those that can be seen by the naked eye. There is only one type of megascopic feature formed by the passage of shock waves, which can be considered a sure proof of impact. These features are called shatter cones (French & Koeberl 2010).

3.3.1 Shatter cones

In addition to being the single megascopic, impact diagnostic, shock deformation feature, shatter cones are also the only shock diagnostic feature that can be formed by pressures as low as 2 GPa.

Shatter cones are made up of several sets of curved, striations penetrating the target rock, creating a cone-like pattern (Fig.4; French 1998). The size of a separate cone can vary from millimetre- to meter scale (French 1998). Shatter cones were the first types of shock features proposed as a diagnostic criterion to impact structures and still play an important role in identifying new impact structures (French & Koeberl 2010). Since shatter cones form at a fairly large interval of shock pressure, approximately 2 GPa to 30 GPa, they can be found throughout a large volume of the target rock (French 1998). Shatter cones are probably formed as a direct result of the passing shock wave (French & Koeberl 2010), however the exact mechanisms behind the formation of shatter cones are not yet completely understood (French 1998).

Shatter cones can be found in several types of rocks and their morphology varies with different types of host rocks (French 1998).

3.4 Microscopic features

On a microscopic scale, traces of impacts can be found as a collection of microscopic deformation features.

Fig. 4. Shatter Cone. Medium sized shatter cones in limestone. Distinct striations diverging from individual cone

Shock effects that can be seen in a petrographic microscope comes in forms of; selective mineral melting, diapeltic glasses, mosaicism, and a collection of microscopic deformation features such as planar microstructures.

3.4.1 Planar structures

Planar structures is a collective term referring to planar fractures and planar deformation features, PDFs, created by shock waves. They form as a result of partial, localized deformation of the host mineral. Classification of planar structure is mainly based on shock features in quartz (Stöffler 1971; Grieve & Stöffler 2007). Planar structures are generally formed at shock pressures ranging between >7 Gpa to 35 GPa, with PDFs forming at about 10-35 GPa (Stöffler 1971).

3.4.2 Planar fractures (~5-8 GPa)

Planar fracturing is a plastic deformation feature that has been observed in several types of shocked minerals (stöffler 1971). They can be seen as "more or less irregular sets of parallel fractures" (Stöffler 1971). Planar fractures usually have a relatively wide spacing, often more than 20mm (Fig. 5; Stöffler 1971; Stöffler & Langenhorst 1993) Planar fractures are formed at shock pressures ranging from approximately 5-8 GPa (French 1998). These features are possibly formed by plastic and elastic shock and can therefore not be used as sure proof of an impact event, even though they are often found accompanied by unambiguous shock features (Stöffler 1971).

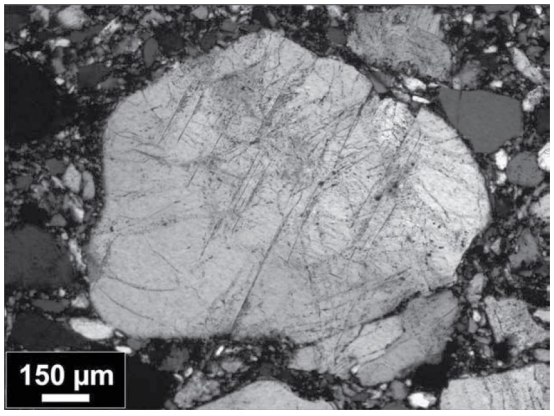

Fig. 5. Planar fractures, PF. Planar fractures in quartz grain. From French & Koeberl 2010.

3.4.3 Planar deformation features (~10-35 GPa)

Planar deformation features, or PDFs, are one of the shock metamorphic features that are exclusively formed by the passing of high-energy shock waves. The uniqueness, frequent occurrence and easily recognizable nature of PDFs have made them the most popular shock effect used when identifying new impact structures (French & Koeberl 2010). PDFs have been observed in most important rock forming minerals such as quartz, feldspars pyroxenes and amphiboles (French 1998). However, PDFs formed in quartz have been studied to a much higher extent and in greater detail than in any other mineral. The reason for this is partly that the crystal structure in quartz is less complicated than those of feldspars and amphiboles. Further, most studies on shocked rocks has been carried out on solid crystalline rock, which normally has a high occurrence of quartz, which in turn offers a quicker and simpler way to determining an impact origin (French 1998). Quartz is also a generally more durable mineral, less prone to weathering and associated secondary alteration, making it more accessible for petrographic studies.

PDFs tend to form along specific planes within the crystal lattice, by measuring the orientation of the PDFs it is possible to tell the true PDFs apart from other planar features (French 1998). In quartz, PDFs come in narrowly spaced groups, or sets. PDFs in quartz are classified into two types; fresh and decorated. The latter one is formed by thermal annealing, which leaves the PDFs hosting gas inclusions, or bubbles.

In this study similar structures found in feldspars will also be referred to as PDFs.

3.4.4 Deformation bands

Deformation bands were described by Stöffler (1971) as; "Any lamellar-shaped region in a crystal whose orientation differs from that of the crystal". According to the definition of Carter et al. 1964, the formation of deformation bands are the result of lattice gilding during plastic deformation. Given this definition, mechanical twins and kink bands are both classified as deformation bands.

3.4.5 High-pressure mineral polymorphs (~10-15 GPa)

Mineral polymorphs such as coesite and diamonds are normally produced from endogenic processes, deep within the Earth (>60km depth). They can however also form in near-surface rocks during impact events. During impacts, quartz can begin to morph into coesite at shock pressures just exceeding 2 GPa, and to stitshovite at around 10-15GPa. Interestingly enough, during normal geological deformation in the earths crust, quartz requires only half the pressure to convert into stitshovite (>12-15 GPa) than it does to turn into coesite (>30 GPa) (French 1998).

3.4.6 Shock mosaicism

Shock mosaicism is an optical phenomena expressed as a generally chaotic extinction under a petrographic microscope. Shock mosaicism is caused by disorientation of the minerals crystal structure. This feature is not diagnostic since weaker forms of mosaicism can be produced by normal geological processes (Grieve & Stöffler 2007).

3.4.7 Diapletic glass (~35-45 GPa)

Diapletic glasses most commonly forms from feldspars or quartz as a result of shock pressures exceeding 30 GPa (30-50 GPa) (French & Koeberl 2010). It is an amorphous crystal phase produced directly by the shock wave, without preceding melting of the mineral (French & Koberl 2010). Since there is no melting or flowing involved, diapletic glasses normally have most of the original minerals fabric and textures intact. Diapletic glasses formed from quartz and feldspars can be recognized in a petrographic microscope through their isotropic nature (French 1998)

3.4.8 Selective mineral melting(~35-45 GPa)

Selective mineral melting can often found in close connection to the formation of diapletic glasses, at the top end of the pressure range for diapletic glass formation, approximately 45-50 GPa (French 1998).

Post-shock temperatures can reach up to well

over 1000°C which is above the melting point of many common minerals. Minerals within the target rock will respond to the shock pressure individually. Depending to a minerals specific compressibility the post shock temperature will alter from mineral to mineral, if the temperature exceeds the one mineral's melting point that mineral will immediately melt. This individual melting creates an unusual texture made up of melted minerals next to non-melted ones.

4 Material & methods

This study is based on three samples of target rock collected from different locations in the Siljan area.
The samples were prepared to thin sections and then studied with a polarization microscope.

The focus of the study was to examine the general appearance of the k-feldspars, potential occurrence of shock deformation features and possible variations between the different samples. The samples are derived from areas within different peak pressure zones. The shock zonation for the individual samples have previously been established by Holm et al. 2011, based on PDFs in Quartz.

4.1 Geological setting

The approximately 52km wide Siljan impact structure is located in South-central Sweden. The structure can be found at the border where the felsic intrusive Transcandian Igneous Belt meets older Svecofennian rocks (Högdahl et al.2004). The central area mainly consists of Dala-granites, however some mafic intrusive, extrusive magmatic and sedimentary rocks can also be found within this area, for information of regional geology of the Siljan area, the reader is referred to; (Kresten & Aaro 1987), and (Hjelmqvist 1966). The structure itself is heavily eroded which has lead to the exposure of formerly deep-seated levels originally located below the crater floor (Holm et al. 2011). The structure has been dated to 377± 2Ma (Reimond et al. 2005). For more detailed information about the geological setting of the Siljan impact structure the reader is directed to the publication by Holm et al. 2011.

5 Results

Several microscopic deformation features were observed in the studied samples. The majority of the deformation features were found in sample 66, the sample from the zone with the highest estimated pressure range. Sample 51 was highly altered and no deformation features could be positively identified.
The occurrences of shock metamorphic features in the studied samples are summarized in Table. 1.

5.1 Description of samples

All the samples are composed of Järna granite (Holm et al 2011). Sample 21 is derived from an area very close to where the Järna granite meets the Siljan granite (Kersten & Aaro 1987, Kresten et al. 1991), which means that some variations in lithology not apparent on the bedrock map (Kersten & Aaro 1987, Kersten et al. 1991) is possible. All three samples contain varying concentrations of the following minerals; k-feldspars, plagioclase, quartz, biotite, hornblende, titanite and opaques. A more detailed description of the studies samples follows below.

5.1.1 Sample 66

Estimated pressure for this sample range between 15-20 GPa (Holm et al. 2011). The sample has a generally high concentration of feldspars. Approximately 85-90% of the grains are feldspars and a majority of those are k-feldspars. The level of alteration varies from grain to grain, most plagioclase grains are highly altered and can be easily recognized by their brownish colour in uncrossed polarized light. Grain sizes vary within the sample.
All quartz grains observed in the sample hosted PDFs. The frequency of shock features within the k-feldspars in this sample has been estimated to 90-100%, though secondary alteration of the grain surfaces obstruct correct estimation.

5.1.2 Sample 21

Estimated pressure for this sample range between 10-15 GPa (Holm et al. 2011). The minerals in this sample are affected by alteration, but in general to a lesser extent than in sample 66. The thin section from sample 21 contains a much higher percentage of quartz than sample 66 and most grains are in general much larger. The k-feldspars are especially large and relatively few in number, together the three largest k-feldspar grains make up approximately 25% of the entire thin section. In comparison the largest k-feldspar grain observed in sample 66 approximately takes up a mere 5% of the total surface.

5.1.3 Sample 51

Estimated pressure for this sample range between 10-15 GPa (Holm et al. 2011). This sample is highly altered to the extent that observation of any planar features has been extremely difficult. The surface of the feldspars is generally very dark brown. The original twinning within the k-feldspars has been deformed, making it hard to tell twin-features from possible shock features. Grain sizes and mineral distribution appears to be similar to that of sample 66.

5.2 Description of microscopic deformation features observed

5.2.1 Deformation bands

Deformation bands have been observed in various places throughout the thin section from sample 66. They appear as relatively broad, white, band that can be seen in both crossed– and uncrossed polarized light

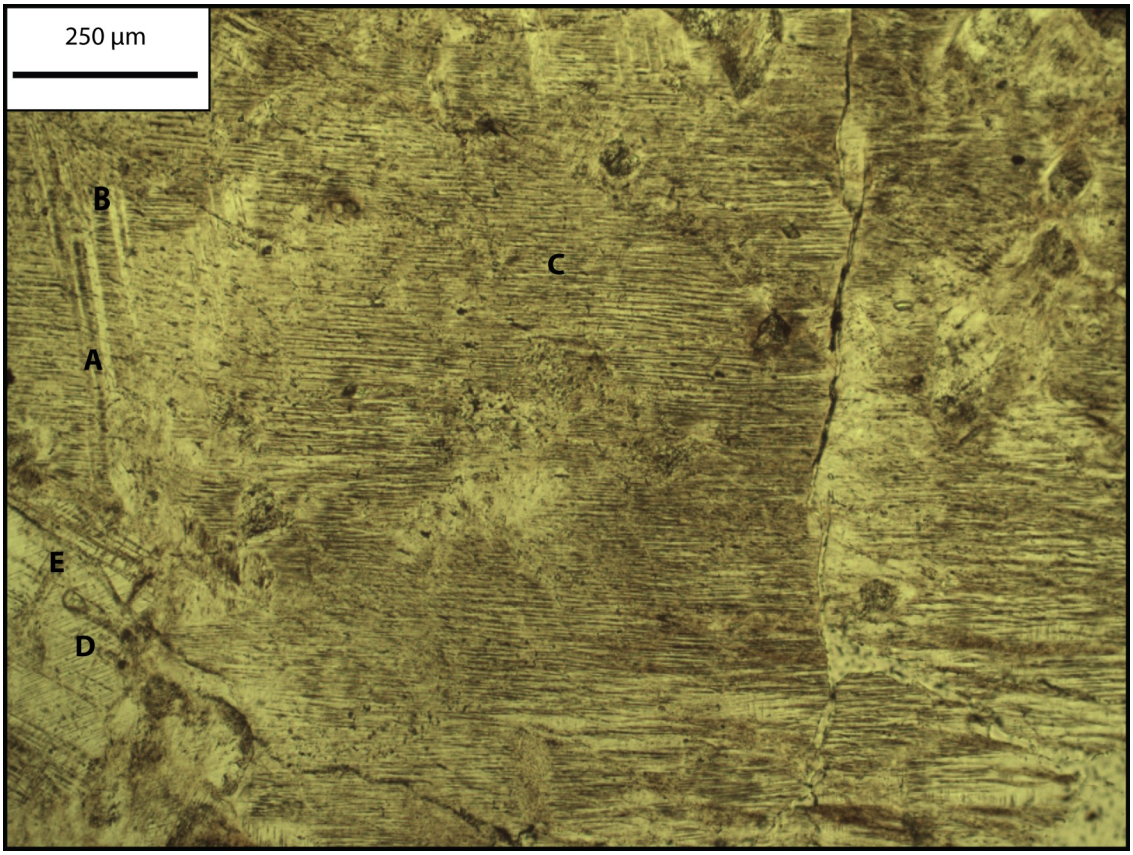

Fig. 6. Microscopic shock deformation features in k-feldspar grain. Photomicrograph uncrossed polarizers. 100X magnification. **A.** Deformation bands. **B.** Ladder texture. **C.** Long deformation features **D.** Planar deformation features, PDFs. **E.** Alteration along the planes of orignal twinning.

(Fig. 6,7,8,9). Most observed deformation bands are slightly crooked, although some almost entirely straight "sets" has been observed. These straight sets of deformation bands are generally shorter and thinner than the curved type.

The deformation bands normally occur together, usually no less than 4 bands per "set". Within the sets the width of the bands vary between approximately 10-20 µm, and spacing between lines: 1-30 µm. The length of the bands ranges from 100 up to approximately 700µm. The more curved type of deformation bands fit the description of deformation bands given by Bunch 1968; "The deformation bands are narrow and tends to pinch out".

5.2.2 Planar deformation features, PDFs

The features referred to as PDFs in this study are similar to PDFs found in Quartz in the way of being very thin, short and closely spaced lines that occur in sets of varying direction (Fig 6,9). The PDFs found in sample 66 and 12 appear to have brownish colour, this could be a result of secondary alteration (French 1998).

The PDFs are often accompanied by the "long planar microstructures" which is a very common feature in this sample.

5.2.3 Ladder texture

A ladder texture is created through the combination of PDFs together with deformation bands or original twinning (French 1998). The thinner, more closely spaced lines of the PDFs positioned in between two thicker, more widely spaced deformation bands or twinning at right angles to each other, this create a features that resembles a ladder (Fig.6). In this study both twinning and deformation bands have been observed to create ladder textures. In most places the PDFs have been replaced by the feature referred to in this study as *long deformation features, LDFs* (Fig. 6, 8).

5.2.4 Long deformation features, LDFs

Features much similar to the PDFs in regard to spacing and width. LDFs are the most frequently observed feature in sample 66. They occur roughly in about 70 percent of the k-feldspars. The most obvious difference between these features and the PDFs are that they are much longer than the PDFs, often stretching over the length of an entire grain. The direction is normally constant within a grain, though some variations have been observed .

LDFs can be considered to come in sets of

internally more narrow spacing, yet all separate sets normally share the same direction within a grain. The banding can be somewhat wavy, in addition to discrete changes in direction, the features can give a rather chaotic impression. Individual lines are often abruptly terminated, only to be replaced by another line in very close connection. These features can be seen in both crossed– and uncrossed polarized light. The LDFs do not seem to be affected by the original twinning in any way. Features occurring in the same direction as the original twinning has been disregarded in this study.

5.2.5 Planar fractures

Described by Grieve & Stöffler 2007 as multiple sets of planar fissures parallel to rational crystallographic planes.

The structures observed in this sample appear to be somewhat brighter than other features observed in the same grain. The fractures observed do not come in sets (sets meaning multiple groups of tightly spaced lines), but rather as individual parallel lines occurring throughout the entire grain (Fig. 8). The spacing varies through the grain; typical spacing ranges between 50-100 µm. The fractures typically occur perpendicular to the LSTS or PDFs. The length of the fractures ranges somewhere between 100-150µm, the width rarely exceed 10 µm. These features are not very abundant but have been observed in a number of grains.

5.2.6 V-Texture

No earlier references or analogues to this feature have been found in earlier publicized studies. This features which, in this study, will be referred to as "V-texture" is composed of thin dark and light streaks, very much resembling short deformation bands. The spacing and thickness of the lines can vary within an individual "v-feature". The size of a single v-feature varies largely from as small as 15µm up to 500µm. The V-shape is constructed of streaks trending in different directions, terminating as they join at the apex of the "V" (Fig 7). The spacing between the streaks varies between around 15-20µm and the width of individual streaks are usually 10µm.

	Sample 66	**Sample 21**	**Sample 51**
Estimated pressure range	15-20 GPa	10-15 GPa	10-15 GPa
Shocked feldspars	X	X	X
Percent shocked feldspar	~90-100%	~50- 60% (or less)	Not observed
Deformation bands	X	Not observed	Not observed
Planar fractures	X	Not observed	Not observed
LDFs	X	X	Not observed
PDFs	X	X	Not observed
Ladder-texture	X	Not observed	Not observed
V-texture	X	Not observed	Not observed

Tabel. 1. Summary of microscopic deformation features observed in samples. Estimated pressure range for each sample, features observed in individual sample, percent of shocked feldspar in each sample.

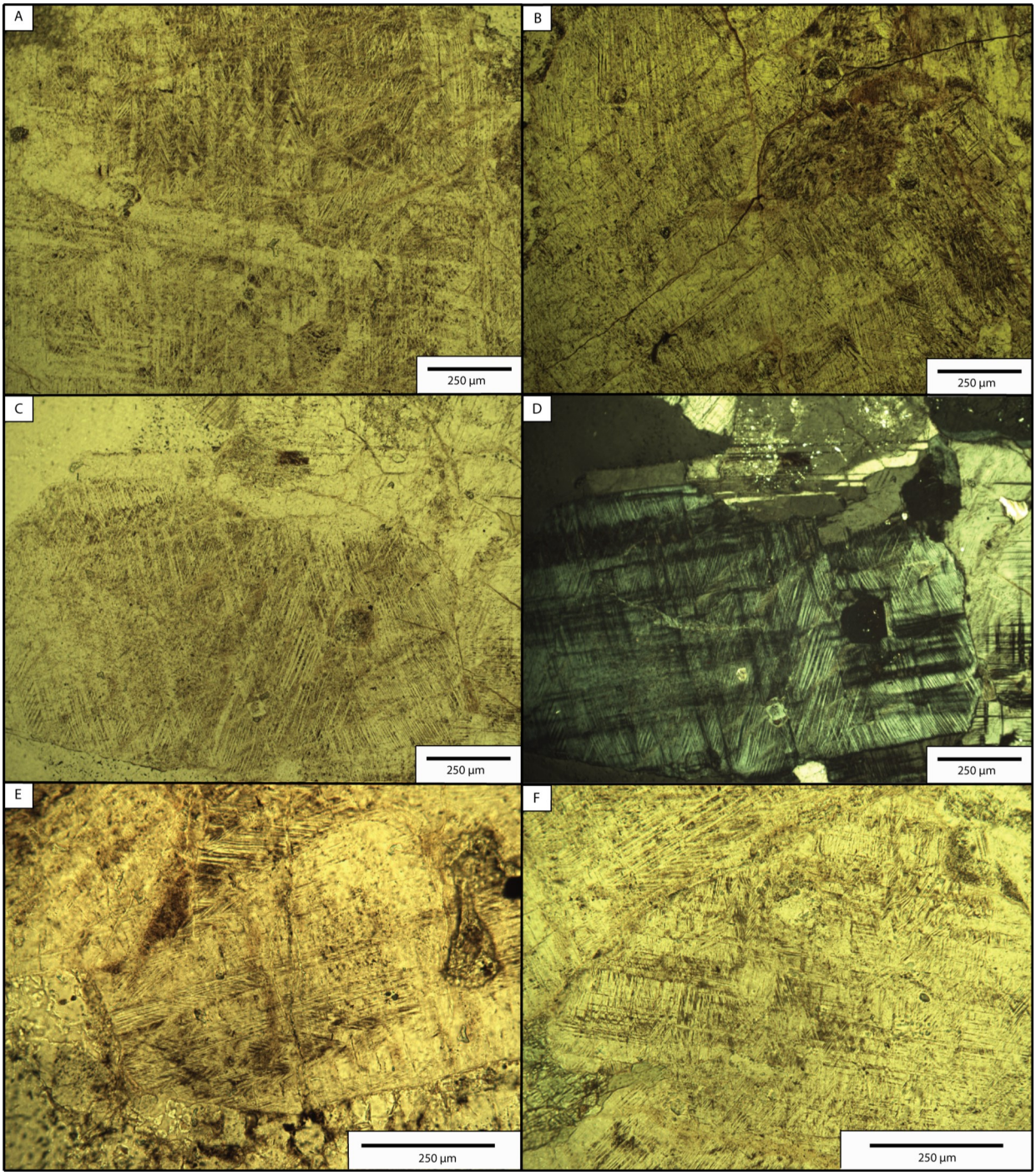

Fig. 7. V-texture and crossed deformation bands. Photomicrographs from sample 66. **A.** V-textures visible especially in the centre of the grain, very large ~ 500µm long features can be seen at the right side of the picture. 100X magnification (uncrossed polars). **B.** V-textures can be observed at the right side of the picture 100X magnification (uncrossed polars). **C.** Long deformation bands trending NE/SW and NW/SE crossing with apexes pointing north. 100X magnification (uncrossed polars). **D.** Showing picture C taken with cross-polarized light. **E.** V-texture can be seen in the grain centre, apexes pointing ENE. 100X magnification (uncrossed polars). **F.** Faint V-textures can appears throughout the grain, apexes pointing North. 100X magnification (uncrossed polars).

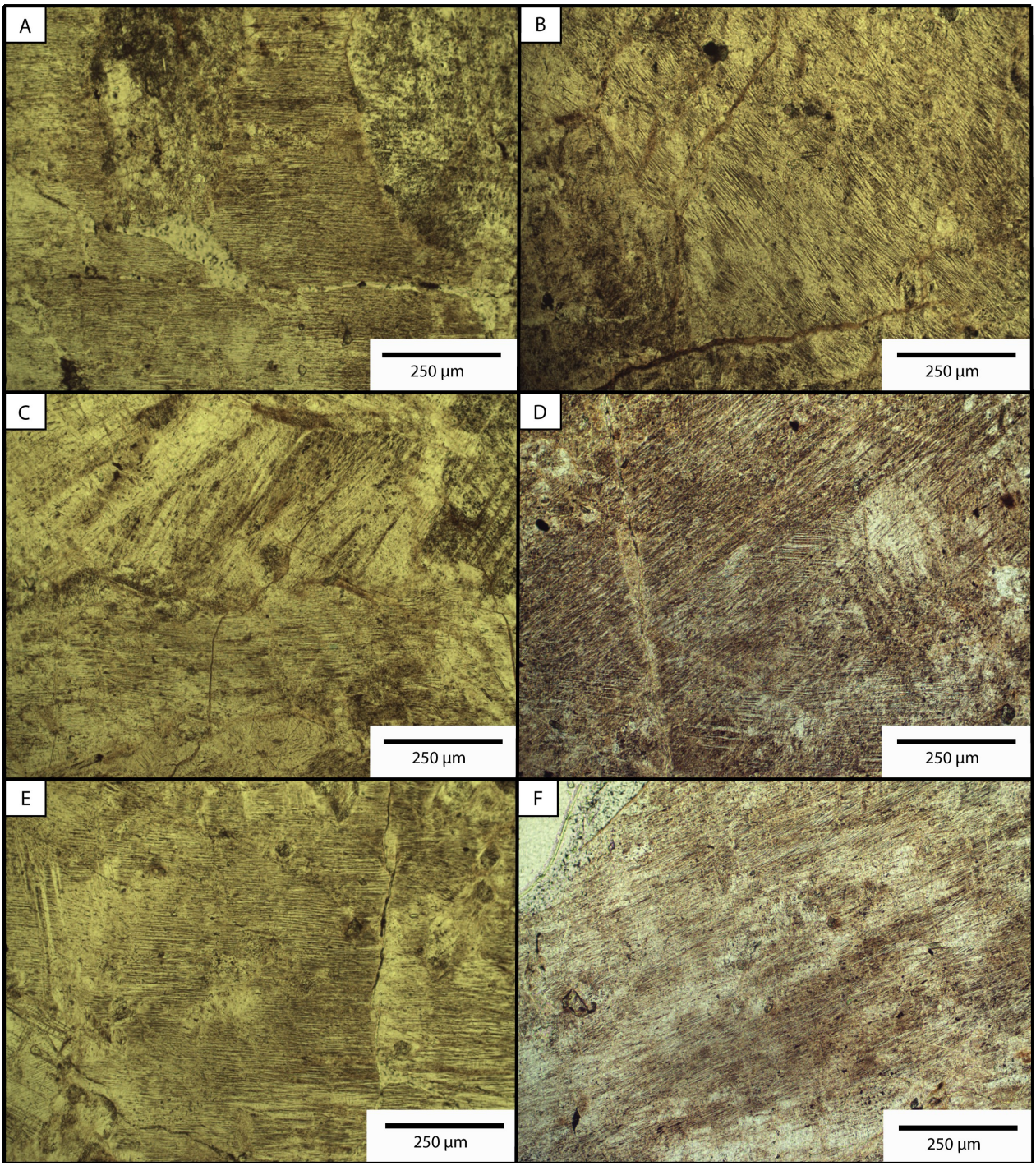

Fig. 8. Long deformation features, LDFs. Photomicrographs of k-feldspars from sample 66, 100X magnification uncrossed polars. **A.** Very thin LDFs can be seen trending E/W stretching throughout the grain. **B.** LDFs Can be seen trending NW/SE, prominent in the left side of the picture. Thickness varies throughout the grain, compare the lower right side to central parts. Features very much resemble thin deformation bands. Short, narrow banding, possible PDFs, can be seen trending WNW/ESE, just above the fracture in the lower part of the picture. **C.** Slightly curved LDFs. Can be seen trending E/W in the centre of the image. Just like in B, the banding varies in thickness looks very similar o deformation bands. The light features trending NE are most possibly twin-related. In the lowest part of the picture NW trending very thin banding can also be seen, possible PDFs. **D.** Long deformation features trending NE/SW throughout the grain. Also thin, slightly curved deformation bands trending E/W can be seen at the centre and lower part of the picture. **E.** Long deformation features trending E/W, "transforming" into clear deformation bands in the lower part of the picture. PDFs, trending NE/SW in the lower left corner. Deformation bands trending N/S on left hand side of picture, creating a ladder structure in combination with the LDFs. See Fig. 6. for larger image. **F.** LDFs trending NE/SW, possible planar fractures, PFs, trending almost N/S.

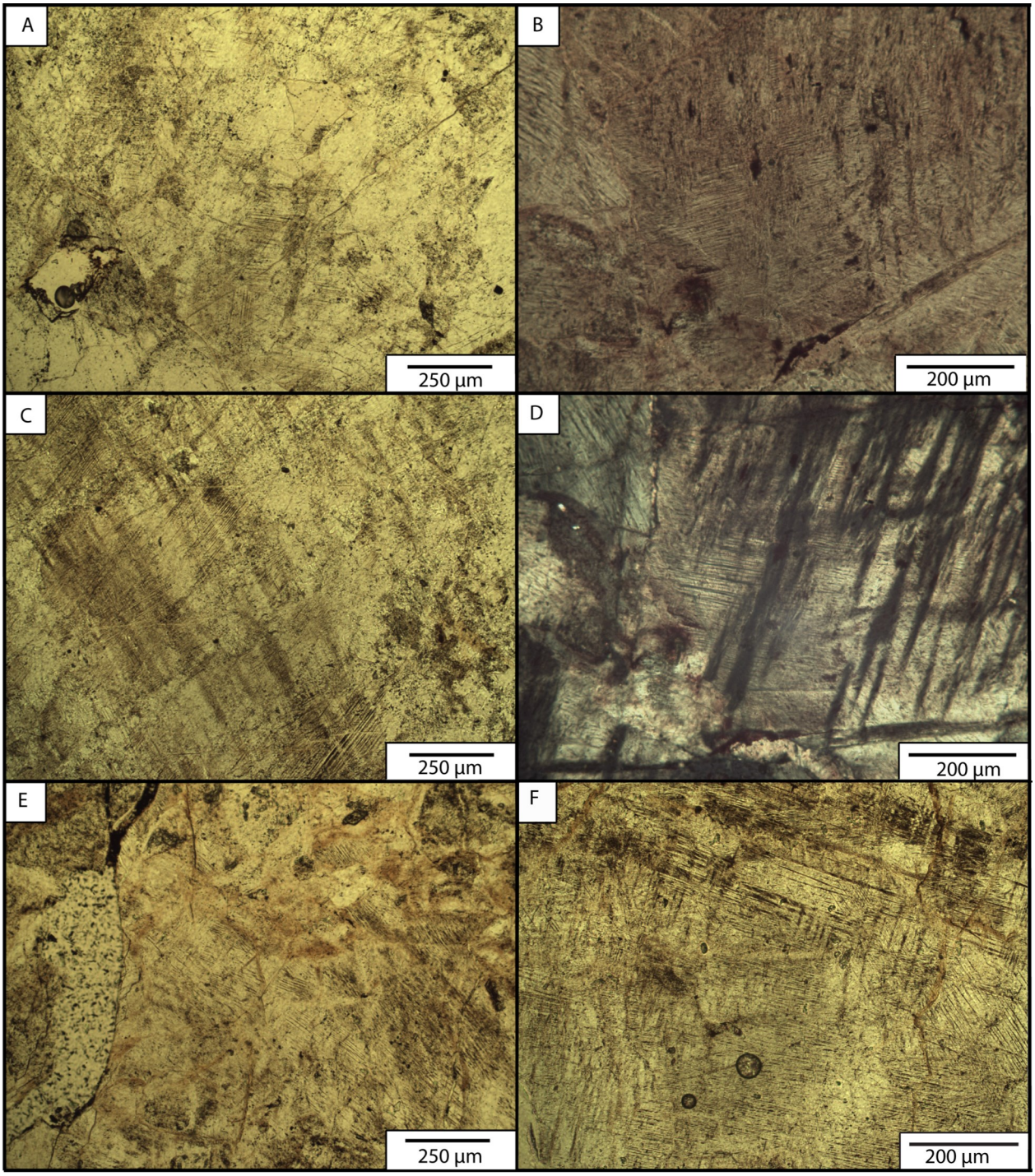

Fig. 9. Planar deformation features, PDFs. Photomicrographs of k-feldspars from sample 66. **A.** At least two sets of possible PDFs, trending N/S and E/W. 100X magnification (uncrossed polars). From sample 21. **B.** Set of possible PDFs trending WNW/ESE. 200X magnification (uncrossed polars). From sample 66. **C.** Trending NE/SW, SE/NW, NEN/SWS are three sets of possible PDFs in k-feldspar from sample 21. 100X magnification (uncrossed polars). **D.** Same grain as shown in figure B, taken with crossed polars, 200X magnification. From sample 66. **E.** K-feldspar with multiple isolated sets of PDFs with slightly diverging direction. Deformation bands trending NW/SE cab be seen at the right side of the picture. From sample 66 (uncrossed polars). **F.** Possible PDFs can be seen at the right side of the image, trending NW/SE, long deformation features can also be seen trending S/E in the lower part of the image. 100X magnification (uncrossed polars).

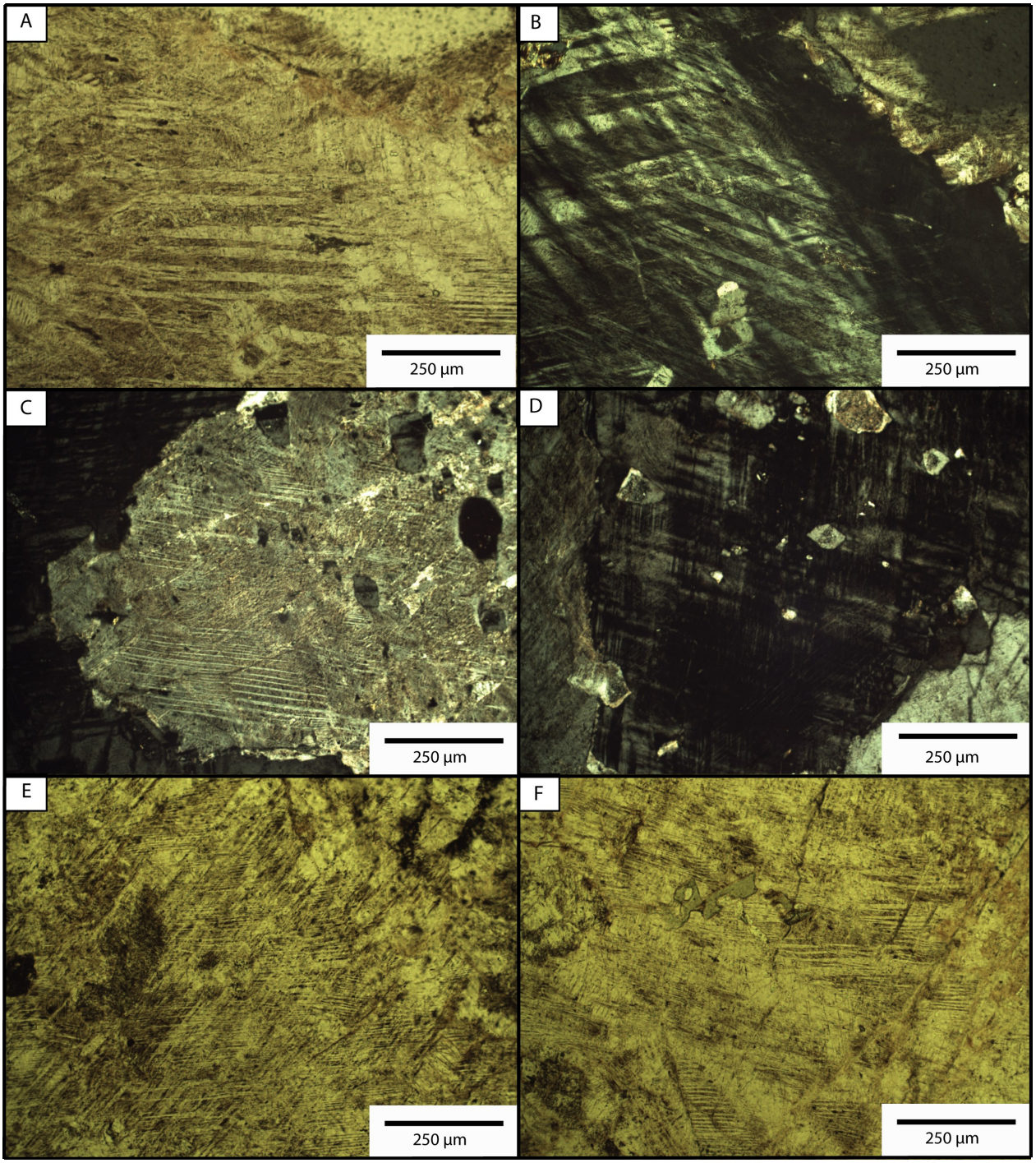

Fig. 10. Deformation bands. Photomicrograph of k-feldspars from sample 66. 100X magnification. **A.** Very thick deformation bands trending E/W, pinched out at the ends (uncrossed polars). **B.** Same features as in A, original twinning can be seen trending NW/SE (crossed polars). **C.** Thinner type, slightly curved deformation bands trending E/W (Crossed polars). **D.** Same features as shown in C, rotated ~45°, deformation bands can be seen to extinguish (crossed polars). **E.** Thin deformation bands can be seen trending E/W (uncrossed polars). **F.** Deformation bands trending E/W, the deformation bands are terminated abruptly in connection to the light areas in the centre of the picture. Light areas appear to be connected to original twinning. (uncrossed polars).

6 Discussion

From studying the three samples from Siljan impact crater it is clear that sample 66, which has been exposed to a higher level shock pressure (15-20 GPa) hosts a much larger number, and a greater diversity of deformation features than sample 21 from the lower shock level (10-15 GPa). Since this study only covers three samples from the different shock levels the possibility that this difference might have been a coincidence can not be disregarded. There are also some variations in grain sizes of the granitic rock in sample 21 and 66, which could in some way be a contributing factor to the difference in number of deformation features observed. Sample 51 were unfortunately too affected by secondary alteration to offer any possibility to observe any deformation features.

A challenging part of the study has been to identify the different features observed in the samples. Earlier publications of studies with focus on microscopic deformation features in k-feldspars are scarce, which limits the possibility to compare observed features with earlier findings. In this study the term "long deformation features" and "V-texture", have been used to refer to features for which no satisfying description from earlier publications have been available.

The features referred to as "long deformation features, LDFs" have many similarities to both PDFs and some of the variations of deformation bands observed in this study. Especially the thicker type of LDFs are similar to the thinnest type of deformation bands and it is possible that LDFs, or at least some of the features referred to as LDFs could be variations of deformation bands. It should also be noted that LDFs often occur together with obvious deformation bands. However, the LDFs have not been observed to extinguish or be affected by the original twinning, which is not the case for the deformation bands (Fig. 10; B,D,F).

There is also another uncertainty regarding the deformation bands. The large variation in width and general appearance might suggest that there might be two different types of deformation bands, they might even be considered as two separate features.

To be able to determine shock pressure regimes in a target rock, based solely on microscopic shock features in feldspars, further detailed studies are necessary. The focus of these studies could include comparisons between shock-induced microscopic features in feldspars and features created by tectonic deformation, similar to the study based on quartz made by Vernooij & Langenhorst (2005).

Further, studies of shock features in different types of feldspars, such as the experimental study carried out by Ostertag (1983), would broaden the field of application and advance the accuracy of future interpretations. However without a detailed classification of microscopic deformation features in feldspars the use of information from experimental studies will be aggravated by the sheer lack of common applicable terminology. A description of some deformation features can be found in Stöffler 1971, where planar fractures, mosaicism, deformation bands and planar elements are introduced. However the description refers to features found in a number of common rock forming minerals and not specifically feldspars.

A more specified, feldspar-orientated, study would be useful to create a satisfying and applicable classification of microscopic shock deformation features created in feldspars.

7 Conclusions

1. Microscopic shock metamorphic features have been observed in k-feldspars from Siljan impact structure.

2. A larger frequency and diversity of shock features was found in the sample assigned to shock pressure levels ranging from 15-20 GPa than was observed in the sample with shock pressures ranging from 10-15 GPa.

3. Some of the features observed in the samples could not be linked to any deformation features mentioned in earlier publications. These features have been referred to in this study as "Long deformation features" and "V-texture".

4. There is an uncertainty regarding the identification of a majority of the features observed, due to a lack of earlier detailed descriptions of shock deformation features in k-feldspars, and feldspars in general.

5. For future studies a detailed classification of shock deformation features in various types of feldspars is necessary to correctly identify individual microscopic shock deformation features that can be observed in a petrographic microscope.

8 Acknowledgements

I would like to give a big thank you to my supervisor Sanna Alwmark for the great commitment and for all the time spent reading drafts and answering questions. Thank you for all the good advise and help with everything from working the microscope, making photomicrographs, to suggesting relevant literature and providing samples. Also thank you for giving me the opportunity to explore the fascinating subject of shock metamorphism. I would also like to give my thanks to Carl Alwmark for reading drafts and giving valuable suggestions for improvement. Finally thank you Anders Lindskog for all the knowledge, patience and positive energy you provided during the lay-out work.

9 References

Bunch, T.E., 1968: *Some Characteristics of Selected Minerals from Craters*. *In* French, B.M., Short, N.M., (ed.): *Shock Metamorphism of Natural Materials* - Proceedings of the First Conference held at NASA, Goddard Space Flight Center, Greenbelt, Maryland, April 1966. Mono Book Corp. Baltimore. 413-432 pp.

French, B.M., Koeberl, C., 2010: *The convincing identification of terrestrial meteorite impact structures: What works, what doesn't, and why*. Earth-Science Reviews.

French, B. M., 1998: *Traces of Catastrophe - A Handbook of Shock-Metamorphic Effects in Terrestrial Meteorite Impact Structures*. Lunar and Planetary Institute 120 pp.

Gault, D.E., Quaide, W.L., Oberbeck, V.R., 1968: *Impact Cratering Mechanics and Structures*. *In* French, B.M., Short, N.M., (ed.): *Shock Metamorphism of Natural Materials*- Proceedings of the First Conference held at NASA, Goddard Space Flight Center, Greenbelt, Maryland, April 1966. Mono Book Corp, Baltimore. 87-100 pp.

Grieve, R.A.F., Stöffler, D., 2007: *Glossary definitions for impactites*. *In* D. D. Fettes, J. (ed.): *Metamorphic Rocks: A Classification and Glossary of Terms, Recommendations of the International Union of Geological Sciences*. Cambridge University Press.

Hjelmquist, S., 1966: *Beskrivning till berggrundskarta över Kopparbergs län* (Summary description of map of the prequartenary rocks of the Kopparberg county, central Sweden). SGU Ser. Ca. Nr. 40.217p.

Holm, S., Alwmark, C., Alvares, W., Schmitz, B., 2011: *Shock barometry of the Siljan impact structure, Sweden*. Meteoritic & Planetary Science 46, Nr 12.

Högdahl, K., Andersson, U. B., Eklund, O., eds. 2004: *The Transscandinavian Igneous Belt (TIB) in Sweden: A review of its character and evolution*. Geological Survey of Finland Special paper 37. Espoo: Geological Survey of Finland. P. 123.

Kresten, P., Aaro, S., 1987: *Berggrundskartan (Bedrock map) 13E Vansbro N, 13F Falun NV*. SGU Ser. Ai nr 13, nr 15.

Langenhorst, F., Stöffler, D., 1993: Shock metamorphism of quartz in nature and experiment: I Basic observation and theory.

Melosh, H. J., 1989: *Impact Cratering - A Geologic Process*. Oxford University Press, New York. 245 pp.

Ostertag, R,. 1983: *Shock experiments on feldspar crystals*. Proceedings of the fourteenth lunar and planetary science conference, part I. Journal of geophysical research, Vol. 88, Supplement, Pages b364-B376.

Reimond, W.U., Kelley, S. P., Sherlock, S. C, Henkel, H., Koeberl, C., 2005: *Laser argon dating of melt breccias from the Siljan impact structure, Sweden: Implications for a possible relationship to late Devonian extintion events.* Meteoritics & Planetary Science 40:591-607.

Rinehart, J.S., 1968: *Intense Destructive Stresses Resulting from Stress Wave Interactions. In* French, B.M., Short, N.M., (ed.): *Shock Metamorphism of Natural Materials*- Proceedings of the First Conference held at NASA, Goddard Space Flight Center, Greenbelt, Maryland, April 1966. Mono Book Corp, Baltimore. 31-42 pp.

Robertson, P.B., 1975: *Mechanical deformation and structural state of experimentally shock-loaded oligoclases,* Neues Jahrb. Mineral. Monatsh., 6, 255-223 pp.

Vernooij, M. G. C., Langenhorst, F., 2005: *Experimental reproduction of tectonic deformation lamellae in quartz and comparison to shock-induced planar deformation freatures.* Meteoritics & Planetary Science 40, Nr 9/10, 1353-1361.

Stöffler, D., 1971: *Progressive Metamorphism and Classification of Shocked and Brecciated Chrystalline Rocks at Impact Craters*. Journal of geophysical research 76.

Stöffler, D., 1974: *Deformation and transformation of rock-forming minerals by natural and experimental shock processes*, I. Behaviour of minerals under shock compression, Fortschr. Mineral., 49, 50-133, 1972

Tidigare skrifter i serien ”Examensarbeten i Geologi vid Lunds universitet”:

338. Florén, Sara, 2013: Geologisk guide till Söderåsen – 17 geologiskt intressanta platser att besöka. (15 hp)
339. Kullberg, Sara, 2013: Asbestkontamination av dricksvatten och associerade risker. (15 hp)
340. Kihlén, Robin, 2013: Geofysiska resistivitets-mätingar i Sjöcrona Park, Helsingborg, under-sökning av områdets geologiska egenskaper samt 3D modellering i GeoScene3D. (15 hp)
341. Linders, Wictor, 2013: Geofysiska IP-under-sökningar och 3D-modellering av geofysiska samt geotekniska resultat i GeoScene3D, Sjöcrona Park, Helsingborg, Sverige. (15 hp)
342. Sidenmark, Jessica, 2013: A reconnaissance study of Rävliden VHMS-deposit, northern Sweden. (15 hp)
343. Adamsson, Linda, 2013: Peat stratigraphical study of hydrological conditions at Stass Mosse, southern Sweden, and the relation to Holocene bog-pine growth. (45 hp)
344. Gunterberg, Linnéa, 2013: Oil occurrences in crystalline basement rocks, southern Norway – comparison with deeply weathered basement rocks in southern Sweden. (15 hp)
345. Peterffy, Olof, 2013: Evidence of epibenthic microbial mats in Early Jurassic (Sinemurian) tidal deposits, Kulla Gunnarstorp, southern Sweden. (15 hp)
346. Sigeman, Hanna, 2013: Early life and its implications for astrobiology – a case study from Bitter Springs Chert, Australia. (15 hp)
347. Glommé, Alexandra, 2013: Texturella studier och analyser av baddeleyitomvandlingar i zirkon, exempel från sydöstra Ghana. (15 hp)
348. Brådenmark, Niklas, 2013: Alunskiffer på Öland – stratigrafi, utbredning, mäktigheter samt kemiska och fysikaliska egenskaper. (15 hp)
349. Jalnefur Andersson, Evelina, 2013: En MIFO fas 1-inventering av fyra potentiellt förorenade områden i Jönköpings län. (15 hp)
350. Eklöv Pettersson, Anna, 2013: Monazit i Obbhult-komplexet: en pilotstudie. (15 hp)
351. Acevedo Suez, Fernando, 2013: The reliability of the first generation infrared refractometers. (15 hp)
352. Murase, Takemi, 2013: Närkes alunskiffer – utbredning, beskaffenhet och oljeinnehåll. (15 hp)
353. Sjöstedt, Tony, 2013: Geoenergi – utvärdering baserad på ekonomiska och drifttekniska resultat av ett passivt geoenergisystem med värmeuttag ur berg i bostadsrättsföreningen Mandolinen i Lund. (15 hp)
354. Sigfúsdóttir, Thorbjörg, 2013: A sedimentological and stratigraphical study of Veiki moraine in northernmost Sweden. (45 hp)
355. Månsson, Anna, 2013: Hydrogeologisk kartering av Hultan, Sjöbo kommun. (15 hp)
356. Larsson, Emilie, 2013: Identifying the Cretaceous–Paleogene boundary in North Dakota, USA, using portable XRF. (15 hp)
357. Anagnostakis, Stavros, 2013: Upper Cretaceous coprolites from the Münster Basin (northwestern Germany) – a glimpse into the diet of extinct animals. (45 hp)
358. Olsson, Andreas, 2013: Monazite in metasediments from Stensjöstrand: A pilot study. (15 hp)
359. Westman, Malin, 2013: Betydelsen av raka borrhål för större geoenergisystem. (15 hp)
360. Åkesson, Christine, 2013: Pollen analytical and landscape reconstruction study at Lake Storsjön, southern Sweden, over the last 2000 years. (45 hp)
361. Andolfsson, Thomas, 2013: Analyses of thermal conductivity from mineral composition and analyses by use of Thermal Conductivity Scanner: A study of thermal properties in Scanian rock types. (45 hp)
362. Engström, Simon, 2013: Vad kan inneslutningar i zirkon berätta om Varbergscharnockiten, SV Sverige. (15 hp)
363. Jönsson, Ellen, 2013: Bevarat maginnehåll hos mosasaurier. (15 hp)
364. Cederberg, Julia, 2013: U-Pb baddeleyite dating of the Pará de Minas dyke swarm in the São Francisco craton (Brazil) - three generations in a single swarm. (45 hp)
365. Björk, Andreas, 2013: Mineralogisk och malmpetrografisk studie av disseminerade sulfider i rika och fattiga prover från Kleva. (15 hp)
366. Karlsson, Michelle, 2013: En MIFO fas 1-inventering av förorenade områden: Kvarnar med kvicksilverbetning Jönköpings län. (15 hp)
367. Michalchuk, Stephen P., 2013: The Säm

fold structure: characterization of folding and metamorphism in a part of the eclogite-granulite region, Sveconorwegian orogen. (45 hp)

368. Praszkier, Aron, 2013: First evidence of Late Cretaceous decapod crustaceans from Åsen, southern Sweden. (15 hp)
369. Alexson, Johanna, 2013: Artificial groundwater recharge – is it possible in Mozambique? (15 hp)
370. Ehlorsson, Ludvig, 2013: Hydrogeologisk kartering av grundvattenmagasinet Åsumsfältet, Sjöbo. (15 hp)
371. Santsalo, Liina, 2013: The Jurassic extinction events and its relation to CO_2 levels in the atmosphere: a case study on Early Jurassic fossil leaves. (15 hp)
372. Svantesson, Fredrik, 2013: Alunskiffern i Östergötland – utbredning, mäktigheter, stratigrafi och egenskaper. (15 hp)
373. Iqbal, Faisal Javed, 2013: Paleoecology and sedimentology of the Upper Cretaceous (Campanian), marine strata at Åsen, Kristianstad Basin, Southern Sweden, Scania. (45 hp)
374. Kristinsdóttir, Bára Dröfn, 2013: U-Pb, O and Lu-Hf isotope ratios of detrital zircon from Ghana, West-African Craton – Formation of juvenile, Palaeoproterozoic crust. (45 hp)
375. Grenholm, Mikael, 2014: The Birimian event in the Baoulé Mossi domain (West African Craton) — regional and global context. (45 hp)
376. Hafnadóttir, Marín Ósk, 2014: Understanding igneous processes through zircon trace element systematics: prospects and pitfalls. (45 hp)
377. Jönsson, Cecilia A. M., 2014: Geophysical ground surveys of the Matchless Amphibolite Belt in Namibia. (45 hp)
378. Åkesson, Sofia, 2014: Skjutbanors påverkan på mark och miljö. (15 hp)
379. Härling, Jesper, 2014: Food partitioning and dietary habits of mosasaurs (Reptilia, Mosasauridae) from the Campanian (Upper Cretaceous) of the Kristianstad Basin, southern Sweden. (45 hp)
380. Kristensson, Johan, 2014: Ordovicium i Fågelsångskärnan-2, Skåne – stratigrafi och faciesvariationer. (15 hp)
381. Höglund, Ida, 2014: Hiatus - Sveriges första sällskapsspel i sedimentologi. (15 hp)
382. Malmer, Edit, 2014: Vulkanism - en fara för vår hälsa? (15 hp)
383. Stamsnijder, Joaen, 2014: Bestämning av kvartshalt i sandprov - medtodutveckling med OSL-, SEM– och EDS-analys. (15 hp)
384. Helmfrid, Annelie, 2014: Konceptuell modell över spridningsvägar för glasbruksföroreningar i Rejmyre samhälle. (15 hp)
385. Adolfsson, Max, 2014: Visualizing the volcanic history of the Kaapvaal Craton using ArcGIS. (15 hp)
386. Hajny, Casandra, 2014: Ett mystiskt ryggradsdjursfossil från Åsen och dess koppling till den skånska, krittida ryggradsdjursfaunan. (15 hp)
387. Ekström, Elin, 2014: – Geologins betydelse för geotekniker i Skåne. (15 hp)
388. Thuresson, Emma, 2014: Systematisk sammanställning av större geoenergianläggningar i Sverige. (15 hp)
389. Redmo, Malin, 2014: Paleontologiska och impaktrelaterade studier av ett anomalt lerlager i Schweiz. (15 hp)
390. Artursson, Christopher, 2014: Comparison of radionuclide-based solar reconstructions and sunspot observations the last 2000 years. (15 hp)
391. Svahn, Fredrika, 2014: Traces of impact in crystalline rock – A summary of processes and products of shock metamorphism in crystalline rock with focus on planar deformation features in feldspars. (15 hp)

LUNDS UNIVERSITET

Geologiska institutionen
Lunds universitet
Sölvegatan 12, 223 62 Lund